

SPECTROSCOPIC AND MORPHOLOGIC CHARACTERIZATION OF THE DENTIN/ADHESIVE INTERFACE

R. M. Lemor,[†] M. B. Kruger,[†] D. M. Wieliczka,[†] J. R. Swafford,[‡] and P. Spencer[‡]

[†]University of Missouri–Kansas City, Department of Physics, Kansas City, Missouri 64110; [‡]University of Missouri–Kansas City, School of Dentistry, Kansas City, Missouri 64110

(Paper BVS-02 received July 8, 1998; accepted for publication Sep. 30, 1998.)

ABSTRACT

The potential environmental risks associated with mercury release have forced many European countries to ban the use of dental amalgam. Alternative materials such as composite resins do not provide the clinical function for the length of time characteristically associated with dental amalgam. The weak link in the composite restoration is the dentin/adhesive bond. The purpose of this study was to correlate morphologic characterization of the dentin/adhesive bond with chemical analyses using micro-Fourier transform infrared and micro-Raman spectroscopy. A commercial dental adhesive was placed on dentin substrates cut from extracted, unerupted human third molars. Sections of the dentin/adhesive interface were investigated using infrared radiation produced at the Aladdin synchrotron source; visible radiation from a Kr⁺ laser was used for the micro-Raman spectroscopy. Sections of the dentin/adhesive interface, differentially stained to identify protein, mineral, and adhesive, were examined using light microscopy. Due to its limited spatial resolution and the unknown sample thickness the infrared results cannot be used quantitatively in determining the extent of diffusion. The results from the micro-Raman spectroscopy and light microscopy indicate exposed protein at the dentin/adhesive interface. Using a laser that reduces background fluorescence, the micro-Raman spectroscopy provides quantitative chemical and morphologic information on the dentin/adhesive interface. The staining procedure is sensitive to sites of pure protein and thus, complements the Raman results. © 1999 Society of Photo-Optical Instrumentation Engineers. [S1083-3668(99)00201-4]

Keywords Raman; dentin; interface; diffusion.

1 INTRODUCTION

The potential health and environmental risks associated with mercury release from dental amalgam have forced many European countries to ban the use of this material. In the United States patients are frequently demanding that restorative materials other than dental amalgam be used. These alternative materials, which include composite resins, do not experience the clinical function and longevity that has traditionally been associated with dental amalgam.¹

Under clinical conditions, the retention of composite resins depends on the adhesive bond formed at the tooth/material interface. Although acid-etching provides effective bonding between the composite restoration and treated enamel, there is no treatment currently available to provide a comparable bond at the dentin/material, i.e., the dentin/adhesive interface.² Lack of adhesion at the dentin surface provides a conduit for penetration of bacteria, fluids, and other extraneous substances

between the restoration and the tooth. This exchange of fluids and bacteria at the dentin/adhesive interface can lead to recurrent decay, post operative sensitivity, and breakdown of the bond.³

To date, the majority of investigators has relied on bond strength studies in combination with morphologic examination to identify the myriad of factors that affect bonding at the dentin/adhesive interface. The bond strength studies measure dentin/adhesive reactions primarily at the point of fracture. Morphologic analysis with techniques such as transmission electron microscopy frequently involves specimen preparation that may alter or even destroy the dentin/adhesive interface.^{4,5} Another disadvantage of morphologic techniques is that they provide only limited information on the chemistry of the dentin/adhesive interface. For example, the elemental distribution of dentin can be detected with scanning transmission electron microscopy; to study the adhesive in a similar manner requires "tagging" the resin with an identifying element.⁶

To effectively isolate and identify the factors contributing to failure at the dentin/adhesive interface

Address all correspondence to D. M. Wieliczka, Department of Physics, University of Missouri–Kansas City, 4747 Troost Ave., Kansas City, MO 64110. Tel: 816-235-2505; Fax: 816-235-5221; E-mail: wieliczka@cctr.umkc.edu

Table 1 Description of commercial adhesive ScotchBond Multipurpose Plus.

Product and Manufacturer	Etchant	Primer and Adhesive	Lot No.
Scotchbond Multipurpose Plus	35% phosphoric acid	HEMA (hydroxyethyl methacrylate)	5BU
		Polyalkenoic acid	
3M Corp., St. Paul, MN		BisGMA (bisphenol-A-bis(2-hydroxypropyl methacrylate))	

an understanding of the chemical reactions that occur at these surfaces is needed. The purpose of this study was to characterize the chemistry of the dentin/adhesive interface using micro-Fourier transform infrared (FTIR) and micro-Raman spectroscopy.^{7,8} The chemical results are correlated to morphologic investigation of this interface using a novel light microscopy technique.

2 METHODS AND MATERIALS

2.1 SAMPLE PREPARATION

Extracted unerupted human third molars stored at 4°C in 0.9% w/v NaCl containing 0.002% sodium azide were used in this study. Initial sample preparation proceeded as follows: the occlusal one-third of the crown was sectioned perpendicular to the long axis of the tooth by means of a water-cooled low-speed diamond saw (Buehler, Lake Bluff, IL). The exposed dentin surface was abraded with 600 grit silicon carbide under water, thus creating a uniform smear layer. The prepared dentin was treated with ScotchBond Multipurpose Plus (Table 1) according to the manufacturer's instructions. As per these instructions the dentin is etched for 15 s, washed and dried for 15 s, and the primer and adhesive are applied and polymerized by exposure to visible light (spectrum light, Dentsply, Milford, DE).

Cross-sectioned samples of the dentin/adhesive interface were cut to a thickness of $\sim 3 \mu\text{m}$ using a tungsten carbide knife mounted in a polycut "S" sledge microtome (Leica, Deerfield, IL). These $3\text{-}\mu\text{m}$ -thick sections were used for both the light microscopy and the infrared spectroscopy. The remainder of the bulk sample received no further sample treatment and was analyzed with Raman spectroscopy.

2.2 LIGHT MICROSCOPY

The microtomed sections were collected on glass microscope slides treated with Haupt's adhesive and stained with Goldner trichrome, a classical

bone stain.⁹ Slides with adherent stained sections were dehydrated through ascending ethanol and xylene. The sections were cover slipped with mounting media and examined using a Zeiss light microscope.

In these sections any exposed protein was stained a distinctive red, whereas any mineral therein appeared as green.⁷ Protein that was partially coated with either primer or adhesive was stained orange. The width of the exposed protein layer was determined by direct measurement from photomicrographs whose exact magnification was established with a stage micrometer. The bulk adhesive in these sections was stained pale beige.

2.3 INFRARED SPECTROSCOPY

The $3\text{-}\mu\text{m}$ -thick unstained sections of the dentin/adhesive interface were mounted on silver chloride substrates. The infrared spectra were obtained at the Synchrotron Radiation Center (Stoughton, WI) using the Alladin storage ring operating at an energy of 800 MeV. The infrared spectromicroscopy beamline, port 031, is equipped with a Nicolet Magna-IR 550 FTIR spectrometer coupled with a NIC-Plan microscope. Spectra were acquired from the integration of 256 scans for each sample position, in the range of $700\text{--}4000 \text{ cm}^{-1}$ with a resolution of 8 cm^{-1} . The microscope is equipped with a motorized $x\text{-}y$ stage with $1 \mu\text{m}$ positioning capability and with dual confocal Schwarzschild reflective lenses. The objective lens parameters are 0.58 numerical aperture (NA) $15\times$ and the condenser lens parameters are 0.71 NA $10\times$. The limiting apertures were adjusted to $2\times 18 \mu\text{m}$ (vertical \times horizontal) and oriented to keep the long dimension parallel to the interface. This aperture size provided the maximum signal-to-noise ratio. Spectra were obtained at $1 \mu\text{m}$ intervals across the interface, oversampling the spatial information, with a background spectrum obtained both prior to and at completion of the line scan.

2.4 RAMAN SPECTROSCOPY

Raman spectra were recorded with a Dilor-OMARS 89 Raman spectrometer equipped with an Olympus BH-2 BHT microscope and a liquid nitrogen cooled charge coupled device (CCD) detector, EG&G 1530 C. The excitation source was a Kr^+ laser, operating at 647 nm with power of 50 mW. After passing through the band pass filter and condensing optics, approximately 6 mW was incident upon the sample. Under visual inspection using the Raman microscope attachment, no destructive effects were observed on any of the sample regions. The spectral resolution of the system was 4 cm^{-1} . The sample was placed at the focus of a $100\times$ microscope objective and spectra were acquired at positions corresponding to $1 \mu\text{m}$ intervals using an automated $x\text{-}y$ stage with a spatial resolution of $0.1 \mu\text{m}$. The focus of the laser beam in conjunction with a con-

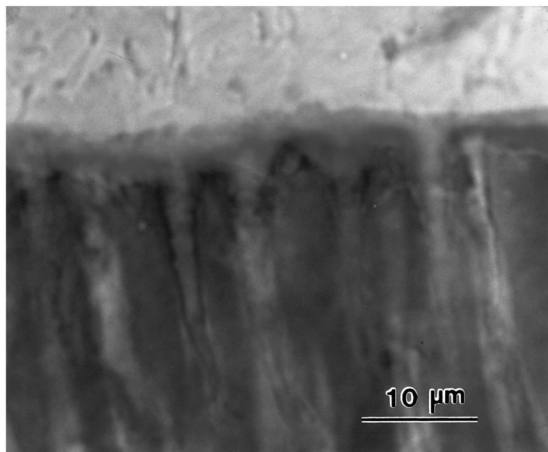


Fig. 1 Light micrograph of the dentin/adhesive interface. The mineralized dentin is stained green, the exposed protein is red, and the adhesive is stained pale beige. The partially coated protein is stained orange.

focal aperture provided a spatial resolution of $\sim 1 \mu\text{m}$. Spectra were obtained by integrating the Raman scattering intensity for 20 min at positions corresponding to $1 \mu\text{m}$ intervals across the dentin/adhesive interface and in three spectral regions, 350–650, 800–1100, and 1475–1700 cm^{-1} . The line scan was obtained from a region devoid of dentinal tubules. After acquisition the data were filtered for spikes and high frequency noise. The composite scans were generated without further modification. Additional spectra from regions of pure dentin and pure adhesive were collected for comparison.

3 RESULTS

3.1 LIGHT MICROSCOPY

A representative light micrograph of a Goldner trichrome stained section is presented in Figure 1. In Figure 1 the mineralized dentin is stained green while the adhesive is pale beige. A distinct red line indicating protein that is exposed and available for reaction with the Goldner trichrome stain can be noted at the dentin/adhesive interface. The width of the red line is $\sim 2 \mu\text{m}$ while the width of the entire red-orange zone is approximately $4 \mu\text{m}$.

3.2 INFRARED SPECTROSCOPY

The infrared transmission spectra for three different positions on the sample are shown in Figures 2(a) and 2(b). Figure 2(a) shows the entire spectral range from 650 to 4000 cm^{-1} and Figure 2(b) shows the range from 750 to 2000 cm^{-1} . The background due to scattering is minimal in the adhesive spectrum, increases in the dentin and is at a maximum in the spectrum taken at the interface. The influence of diffuse scattering from the sample has minimal impact below 2000 cm^{-1} and is most evident in the spectral range from 2000 to 4000 cm^{-1} .

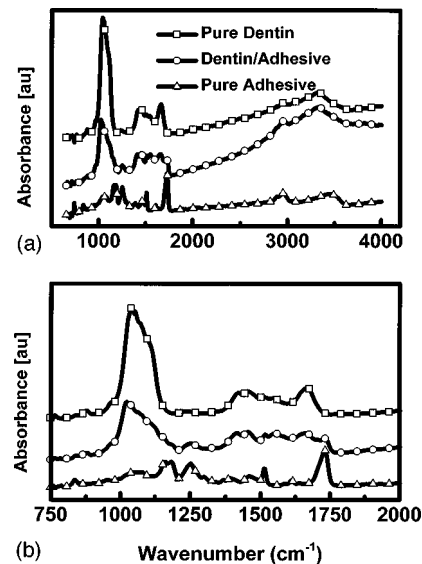


Fig. 2 Infrared absorption spectra for sample regions of pure dentin, the interface and pure adhesive. The spectra have been offset vertically. In (a) the entire spectral range is shown while (b) shows the spectral range from 750 to 2000 cm^{-1} .

Absorption bands attributed to the mineral and protein components of dentin as well as features associated with the adhesive are noted in the spectral range from 750 to 2000 cm^{-1} . Contributions from the mineral phase of the dentin include the orthophosphate band at 900–1160 cm^{-1} and the carbonate band at 875 cm^{-1} . The carbonate band at 1452 cm^{-1} overlaps contributions from the amide II. The absorption bands at ~ 1660 , 1545, and 1245 cm^{-1} , amides I, II, and III, indicate the major protein contributions. The transmission spectrum for the adhesive shows strong features at 1157, 1455, 1510, and 1730 cm^{-1} . These features are tentatively assigned to C—O—C, CH_2 , C_6H_4 , and the C=O ester band.

A composite image of the absorption spectra collected from the dentin/adhesive interface over the spectral range of 750–2000 cm^{-1} is shown in Figure 3. It shows a broad interface, greater than $20 \mu\text{m}$, with a decrease in the mineral and protein signatures accompanied by an increase in the absorption due to the adhesive. Note that the relative decrease in intensity of the orthophosphate band precedes any decrease in intensity of the spectral features associated with the protein. Additionally, none of the absorption lines shift or broaden as a function of position on the sample.

Absorbance data were extracted from the line scans at a given wave number to provide plots of intensity versus position. These data sets were fit to a simple diffusion model described by Wieliczka et al.¹⁰ The concentration, c , at position X given by this model is

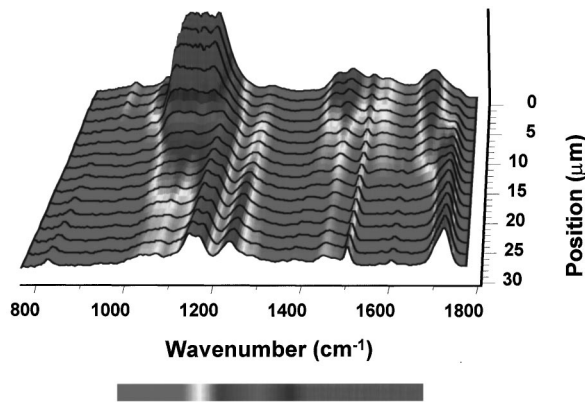


Fig. 3 Composite image of the absorption spectra collected from the dentin/adhesive interface over a spectral range of 750–2000 cm^{-1} and over a linear distance of 30 μm . Red represents low absorbance with purple representing high absorbance.

$$c = \frac{c_0}{2} \left[1 - \operatorname{erf} \left(\frac{x}{2\sqrt{Dt}} \right) \right],$$

where c_0 is the concentration for the pure material, and \sqrt{Dt} is a characteristic length associated with the diffusion at the given interface. The position where the concentration is 50% is defined as the interface position. For the purposes of this work, the concentration of a given component is related to its spectroscopic intensity where the 100% spectroscopic intensity was measured from the pure material a substantial distance from the optical interface. The interface width, defined as the distance between the positions of 10% and 90% intensity, is given by $\Delta X = 3.62\sqrt{Dt}$ with the positions given by $X = \pm 1.812\sqrt{Dt}$. Applying this model to both the dentin/protein and the protein/adhesive interface provides a complete description of the region.

The fit to the diffusion model for the infrared data is presented in Figure 4. The interface width determined by this data set is 20.9 μm with regions of 12.9 μm partially decalcified and 8 μm 100% decalcified. The spectral features associated with the adhesive vary over a distance of 20.4 μm , indicating a sizable overlap of the spectral components associated with the adhesive and mineral. The protein layer, determined by the region between the 50% absorbance levels for mineral and adhesive, is approximately 3.7 μm .

3.3 RAMAN SPECTROSCOPY

The Raman spectra for the three different spectral regions and from positions in pure dentin, the interface, and pure adhesive are shown in Figure 5. Figure 5(a) shows the lower wave number region with broad features at 440–470 and 580 cm^{-1} attributable to both mineral and protein components of the dentin. Within this spectral region the Scotch-Bond Multipurpose Plus adhesive has intense features located at 380, 430, 480, 600, and 635 cm^{-1} .

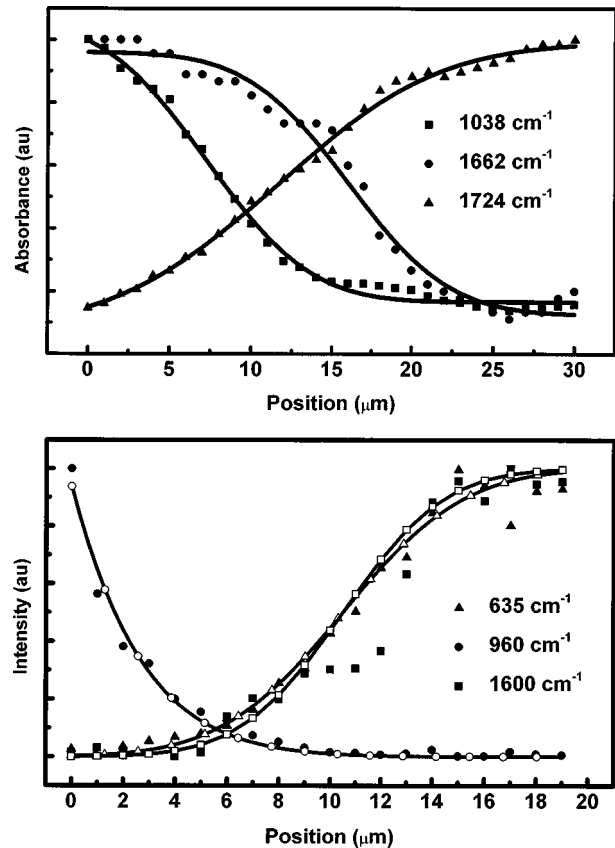


Fig. 4 Fits of the infrared and Raman intensities to the diffusion model. The upper graph shows the fit to the infrared data and the lower the fit to the Raman. The absorbance at 1038, 1662, and 1724 cm^{-1} is due to the mineral, the protein, and the adhesive, respectively. The Raman scattering intensity at 635 and 960 cm^{-1} is due to the adhesive and the mineral, respectively.

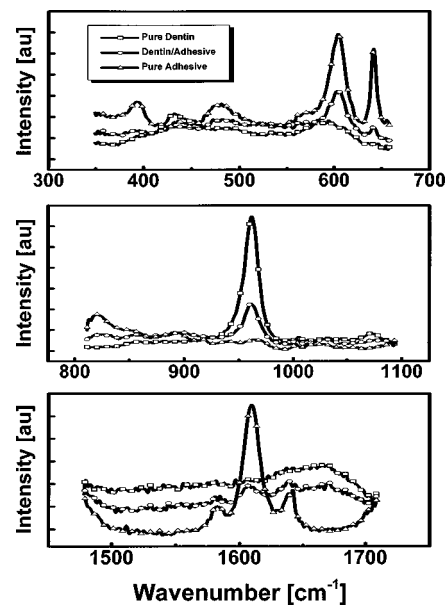


Fig. 5 Raman scattering spectra for the three spectral regions and for sample regions of pure dentin, the interface, and pure adhesive.

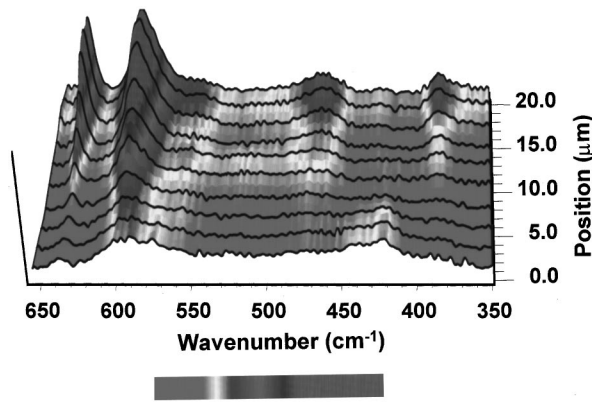


Fig. 6 Composite image of the Raman scattering intensity collected from the dentin/adhesive interface over a spectral range of 350–650 cm^{-1} and over a linear dimension of 20 μm .

The Raman intensity at 635 cm^{-1} was used to monitor the adhesive concentration as a function of position across the interface. The dominant spectral feature in Figure 5(b) is the phosphate group at 960 cm^{-1} associated with the mineral component of dentin. The lack of other structures in this spectral region allowed accurate monitoring of the mineral concentration as a function of position. In Figure 5(c) the three strong peaks at 1580 (phenyl), 1610 (phenyl), and 1640 cm^{-1} (C=C) are associated with the adhesive while the broad weak structure from 1625 to 1700 cm^{-1} is associated with amide I. This was the best spectral region for monitoring the protein composition.

A composite image of the Raman scattering spectra collected from the dentin/adhesive interface over a spectral range of 350–650 cm^{-1} is shown in Figure 6. Again a broad interface is observed, $\sim 20 \mu\text{m}$, with a decrease in the mineral signature accompanied by an increase in the scattering due to the adhesive. Note the gap between the decrease in the adhesive lines at ~ 460 and 380 cm^{-1} and the increase in the scattering from the mineral as shown by the line at $\sim 430 \text{ cm}^{-1}$. The intense lines at ~ 600 and 640 cm^{-1} are associated with scattering from the adhesive.

The fit of the Raman data to the diffusion model is presented in the lower portion of Figure 4. The overall interface width determined by the 90% points for the mineral and adhesive is 14.8 μm . Of this width 6 μm is partially decalcified and 9 μm is 100% decalcified. The zone over which the Raman scattering intensity from the adhesive is changing is 9 μm and it has no direct overlap of the mineral gradient. Finally, using the positions where the adhesive and mineral concentrations become less than 50%, a protein layer of 8.5 μm is determined. Within this layer a region of $\sim 0.5 \mu\text{m}$ has no measurable mineral or adhesive contribution; the remaining portion of the layer, $\sim 8 \mu\text{m}$, has minimal incorporation of these components.

4 DISCUSSION

The majority of current dental bonding systems prepare the dentin using an etchant such as phosphoric acid. Acid etching extracts the mineral phase, radically changing the composition of the dentin. For example, native dentin is 50% (vol %) mineral, 30% protein, and 20% water¹¹ while etched dentin is 30% protein and 70% water.¹² The etched dentin is subsequently treated with an adhesive resin.

The formation of an adequate dentin/adhesive bond depends upon diffusion of the adhesive throughout the demineralized layer and into the unaffected dentin. If the adhesive does not penetrate the demineralized dentin, then the naked protein within this layer will be exposed to oral fluids and vulnerable to degradation by bacterial enzymes. Such degradation can ultimately lead to premature failure of the composite restoration.

In this study, chemical analysis was used in conjunction with light microscopy to identify protein that was exposed as a result of incomplete adhesive penetration. Light micrographs of the Goldner stained sections clearly revealed protein that was not encased in adhesive and, thus, available for reaction with the differential stain. In comparing this result to the infrared and Raman spectroscopic analyses the red-orange zone identifies an area where the adhesive concentration is $< 25\%$.

The quantitative differences, in the results derived from the infrared and Raman spectroscopic analyses, reflect the dissimilar wavelengths of light used in each technique. The absorption bands used to characterize the interface are all in the 1000 cm^{-1} wave number region corresponding to a wavelength of $\sim 10 \mu\text{m}$. The diffraction limit for this wavelength is $\sim 10 \mu\text{m}$ using a single slit diffraction model; thus, absorption data at any given point include information from a much larger region. For example, at the extremes of the map, spectra were acquired from a region within 10 μm of the interface; because of the diffraction limit the acquired spectra include information from the pure adhesive as well as from the interface. Similarly the spectra acquired at the interface is a composite of spectral contributions from pure protein as well as from pure dentin and adhesive on either side of the interface.

Based on the infrared spectroscopy results, the 20 μm interface is an overestimate of the distance over which the chemical composition of the sample is changing. Thus, the fit to the diffusion model using the infrared spectroscopic results can only be used in a qualitative sense. Additionally, the absorbance values cannot be quantified since the variations in sample thickness cannot be determined. Deconvolution techniques could improve the spatial resolution but the instrument function must be known before these techniques can be accurately applied.

In contrast, the Raman spectra were obtained at a wavelength of 647 nm, corresponding to a diffraction limit of 1 μm . Since the interface dimensions are greater than 1 μm , this limitation does not adversely affect the results. For example, the interface width, as evaluated at the positions of 90% Raman scattered intensity associated with the mineral and adhesive, is approximately 15 μm . Using the positions where the Raman intensity is 50% and 25% this width reduces to 8.5 and 4 μm , respectively.

A comparison of the interface dimensions determined with Raman spectroscopy and light microscopy indicate that the staining technique is sensitive to the concentration of the adhesive. That is, the Goldner trichrome interaction is sensitive to the protein/adhesive ratio. Below a 10% adhesive concentration the sample is stained as if the composition were pure protein and between 10% and 25% the stain changes to reflect the contribution from the adhesive. At adhesive concentrations greater than 25% no staining characteristic of protein is observed. The staining technique is insensitive to partial demineralization as observed at the lower boundary of the interface. That is, the light microscopy indicates an abrupt interface whereas the Raman spectroscopy demonstrates a gradual demineralization over a region of approximately 6 μm .

In conclusion, the infrared spectroscopy data provide qualitative information about the dentin/adhesive interface; due to its limited spatial resolution the IR results cannot be used quantitatively. The Raman spectroscopic technique, in combination with a laser that reduces background contribution from fluorescence, provides quantitative chemical and morphologic information on the dentin/adhesive interface.^{10,13} The staining procedure, which is sensitive to sites of pure protein, complements the Raman results. In combination the Raman spectroscopy and light microscopy provide accurate information about the dentin/adhesive interface at the extremes of the composition.

Acknowledgments

This work was supported in part by U.S. PHS Research Grant No. DE-12252-01 from the National Institute of Dental Research, National Institutes of

Health, Bethesda, MD. The Synchrotron Radiation Center is part of the Graduate School of the University of Wisconsin-Madison, and is funded by the Division of Materials Research of the National Science Foundation as a National Facility under Award No. DMR-9531009. The authors gratefully acknowledge the 3M Corporation for donating the dentin adhesive material that was investigated in this project.

REFERENCES

1. F. U. Lutz, I. Krejci, and M. Oddera, "Advanced adhesive restorations: The postamalgam age," *Pract. Perio. Esthet. Dent.* **8**(4), 385-394 (1996).
2. R. J. Meier and J. C. Kresin, "Cavity disinfectants and dentin bonding," *Oper. Dent.* **21**(4), 153-159 (1996).
3. M. F. Chan and J. C. Glynn Jones, "A comparison of four *in vitro* marginal leakage tests applied to root surface restorations," *J. Dent.* **20**(5), 287-293 (1992).
4. H. Sano, M. Yoshiyama, S. Ebisu, M. F. Burrow, T. Takatsu, B. Cuicchi, R. Carvalho, and D. Pashley, "Comparative SEM and TEM observations of nanoleakage within the hybrid layer," *Oper. Dent.* **20**(4), 160-167 (1995).
5. J. Perdigao, P. Lambrechts, B. Van Meerbeek, M. Braem, E. Yildiz, T. Yuel, G. Vanherle, "The interaction of adhesive systems with human dentin," *Am. J. Dent.* **9**(4), 167-173 (1996).
6. J. D. Eick, S. J. Robinson, T. J. Byerley, R. Chappell, P. Spencer, and C. C. Chappelow, "Scanning transmission electron microscopy/energy-dispersive spectroscopy analysis of the dentin adhesive interface using a labeled 2-hydroxyethylmethacrylate analogue," *J. Dent. Res.* **74**(6), 1246-1252 (1995).
7. M. Suzuki, H. Kato, and S. Wakumoto, "Vibrational analysis by Raman spectroscopy of the interface between dental adhesive resin and dentin," *J. Dent. Res.* **70**(7), 1092-1097 (1991).
8. B. Van Meerbeek, H. Mohrbacher, J. P. Celis, J. R. Roos, M. Braem, P. Lambrechts, and G. Vanherle, "Chemical characterization of the resin-dentin interface by micro-Raman spectroscopy," *J. Dent. Res.* **72**(10), 1423-1428 (1993).
9. J. Goldner, "A modification of the Masson trichrome technique for routine laboratory purposes," *Am. J. Pathol.* **14**, 237-243 (1938).
10. D. M. Wieliczka, M. B. Kruger, and P. Spencer, "Raman imaging of dental adhesive diffusion," *Appl. Spectrosc.* **51**(11), 1593-1596 (1997).
11. G. W. Marshall, Jr., "Dentin: Microstructure and characterization," *Quint. Int.* **24**(9), 606-617 (1993).
12. J. D. Eick, A. J. Gwinnett, and D. H. Pashley, "Current concepts of dentin adhesion," *Crit. Rev. Oral Biol. Med.* **8**(3), 306-335 (1996).
13. D. M. Wieliczka, P. Spencer, and M. B. Kruger, "Raman mapping of the dentin/adhesive interface," *Appl. Spectrosc.* **50**(12), 1500-1504 (1996).